ACS OMEGA

Open Access

This article is licensed under CC-BY-NC-ND 4.0

http://pubs.acs.org/journal/acsodf

Article

Silylation-Driven Volatility Enhancement in Mononuclear Calcium, Magnesium, and Barium Complexes with Monomethyl or Silyl Ether and Bis(diketonate)

Chanwoo Park,[#] Seungjin Song,[#] Heenang Choi, Bo Keun Park, Ji Yeon Ryu, Youngkwon Kim, and Taek-Mo Chung*

Cite This: *ACS Omega* 2024, 9, 31864−31870

Read Online

ACCESS | Metrics & More | Article Recommendations | Supporting Information

ABSTRACT: Magnesium, calcium, and barium heteroleptic complexes were synthesized by the substitution reaction of the bis(trimethylsilyl)amide of $Mg(btsa)_2$·DME, $Ca(btsa)_2$·DME, and $Ba(btsa)_2$·2DME with an ethereal group and hfac ligands (btsa = bis(trimethylsilyl)amide, DME = dimethoxyethane). The compounds $Mg(dts)(hfac)_2$ (**1**), $Ca(dts)(hfac)_2$ (**2**), $Mg(dmts)(hfac)_2$ (**3**), $Ca(dmts)(hfac)_2$ (**4**), and $Ba(dmts)(hfac)_2$ (**5**) were fabricated and analyzed using various techniques, including Fourier transform infrared spectroscopy, nuclear magnetic resonance spectroscopy, thermogravimetric analyses, and elemental analysis (dts = 2,2-dimethyl-3,6,9-trioxa-2-siladecane, dmts = 2,2-dimethyl-3,6,9,12-tetraoxa-2-silatridecane, hfac = hexafluoroacetylacetonate). The structures of complexes **2**, **4**, and **5** were confirmed using single-crystal X-ray crystallography; all complexes display monomeric structures. All compounds underwent trimethylsilylation of the coordinating ethereal alcohols (meeH and tmgeH) in the presence of HMDS as byproducts because of their increasing acidity originating from the electron-withdrawing hfac ligands. (meeH = 2-(2-methoxyethoxy)ethan-1-ol, tmgeH = tri(ethylene glycol) monoethyl ether, HMDS = hexamethyldisilazane).

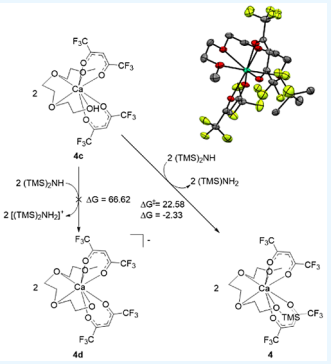

INTRODUCTION

The group two metal compounds containing magnesium, calcium, strontium, and barium are used in various fields, such as magnetoresistive materials, ferroelectrics, piezoelectric materials for dynamic random access memory (DRAM), and as precursors for thin-film growth.[1−10] Electroceramics containing strontium oxide or barium oxide and transition metal oxides, such as $SrTiO_3$, $Ba_{1-x}Sr_xTiO_3$, $BaTiO_3$, $BaSrTiO_3$, and Y-doped $BaZrO_3$, exhibit high permittivity, dielectric constants, and high proton conductivity. However, calcium oxide and magnesium oxide have been used as gate-capacitor dielectrics in metal-oxide-semiconductor field-effect transistors (MOSFETs) and high-electron-mobility transistors (HEMTs). Additionally, magnesium and calcium have been used as optical coating materials for metal fluorides (MgF_2 and CaF_2).[11−19]

The fabrication of thin films containing group two metal oxides or metal fluorides is required for these applications. These metal compounds can be deposited using chemical vapor phase methods, such as metal−organic chemical vapor deposition (MOCVD) and atomic layer deposition (ALD), which require volatile and thermally stable precursors. The development of volatile group two metal compounds is often limited by the formation of oligomeric compounds, particularly strontium, and barium, owing to their large atomic sizes and high coordination spheres.

Sterically bulky ligands or neutral ligands, such as tetraethylene glycol dimethyl ethereal (tetraglyme), tetramethylethylenediamine (TMEDA), β-diketonates, and cyclopentadienyl groups, have been used to address these challenges and synthesize group two metal precursors with saturated metal centers.[20−23] β-diketonates have been used to synthesize group two β-diketonate complexes with high volatility, such as $Mg(tmhd)_2$, $Ca(tmhd)_2$, $Sr(tmhd)_2$, $[Sr(tmhd)_2(triglyme)]$, and $Ba(tmhd)_2$.[24−31] (tmhd = 2,2,6,6-tetramethyl-3,5-heptanedione, triglyme = $Me(OCH_2CH_2)_3OMe$). A previous study observed the tendency of the strontium molecular structure using ethereal ligands with a varying number of oxygen atoms and varying β-diketonate ligands, such as tmhd, acac, tfac, and hfac. When hfacH was used, the hydroxyl hydrogen atom of the ethereal ligand with three or four oxygen atoms was substituted by trimethylsilyl from HMDS and showed high volatility.[32] In this study, ethereal ligands and hfacH were applied to observe alcohol silylation and to synthesize volatile complexes of other two group metals, such as magnesium,

Received: April 10, 2024
Revised: June 21, 2024
Accepted: June 25, 2024
Published: July 11, 2024

© 2024 The Authors. Published by American Chemical Society

https://doi.org/10.1021/acsomega.4c03479
ACS Omega 2024, 9, 31864−31870

Chart 1. Chemical Structures of Ligands Used for Synthesizing Volatile Metal Complexes: (a) Tetraglyme, (b) TMEDA, (c) tmhdH, (d) Triglyme, (e) meeH, and (f) tmgeH

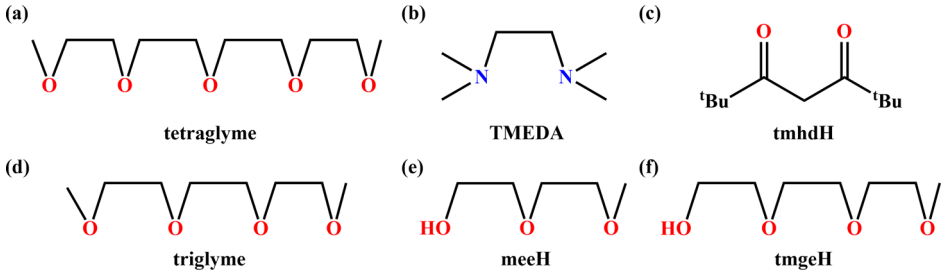

Scheme 1. Synthetic Scheme Complexes 1 and 2

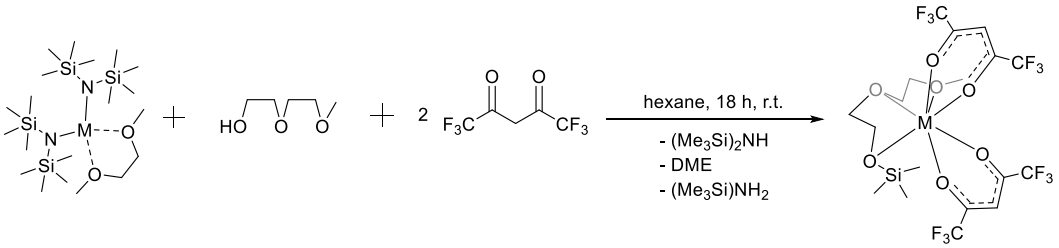

Scheme 2. Synthetic Scheme Complexes 3 and 4

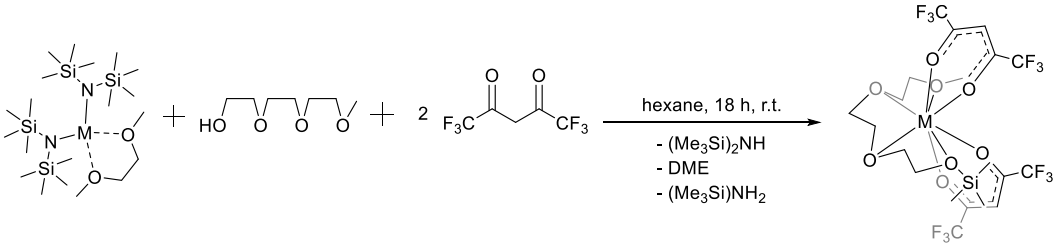

Scheme 3. Synthetic Scheme Complex 5

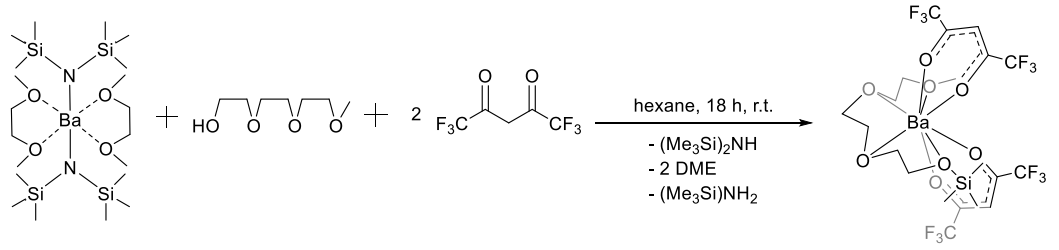

calcium, and barium. Mg(dts)(hfac)$_2$ (**1**), Ca(dts)(hfac)$_2$ (**2**), Mg(dmts)(hfac)$_2$ (**3**), Ca(dmts)(hfac)$_2$ (**4**), and Ba(dmts)-(hfac)$_2$ (**5**) were synthesized by controlled substitution reactions using metal bis(bis(trimethylsilyl amide). In these complexes, compounds **2**, **4**, and **5** were characterized by using X-ray crystallography, and all compounds displayed monomeric structures. DFT calculations were conducted to investigate the alcohol silylation of these complexes, using complex **4** as a reference. The energy differences between each reaction intermediate were calculated to determine the key intermediate in silylation and propose a plausible reaction mechanism for this process. Chart 1 shows chemical structures of general ligands for synthesizng volatile metal precursor.

RESULTS AND DISCUSSION

In this study, new group two metal complexes were synthesized by in situ substitution reactions (Schemes 1–3). Complexes **2**, **4**, and **5** were recrystallized as a white solid from a saturated toluene solution at −30 °C. All complexes exhibited moderate yields of 70−80%. In our previous work, volatile strontium complexes with ethereal ligands have been shown to exhibit various strontium compound tendencies, which are affected by the steric hindrance, electron density, and coordination number of the central metal. When hfacH was added to strontium complexes, the hydrogen atom of ROH was substituted by trimethylsilyl from HMDS; the resulting compound exhibited highly volatile properties.

https://doi.org/10.1021/acsomega.4c03479
ACS Omega 2024, 9, 31864−31870

Therefore, further work was conducted to develop two group metal precursors with improved properties. Group two metal complexes were synthesized using ethereal and hfacH ligands to observe alcohol silylation and investigate their thermal properties as precursors. Similar to strontium complexes $Sr(dmts)(hfac)_2$, other group two metals (magnesium, calcium, and barium) exhibited alcohol silylation from ethereal ligands. In particular, complexes **4** and **5** were sublimed at 100 and 110 °C (1 Torr), whereas complex **1** was distilled at 110 °C (1 Torr). The NMR spectra of the respective complexes were recorded using C_6D_6 as the solvent and a standard at room temperature. In all complexes, the −OH peak was absent; however, the trimethylsilyl peak was observed because of the trimethylsylation of alcohol with HMDS. The CH_3 protons of mee and tmge for complexes **1**, **2**, **3**, **4**, and **5** were observed at δ_H values of 3.02, 2.96, 2.96, 3.10, and 2.97 ppm, respectively. The β-CH protons of the hfac ligand for compounds **1**, **2**, **3**, **4**, and **5** were observed as singlets at δ_H values of 6.20, 6.28, 6.23, 6.31, and 6.29 ppm, respectively. The ^{19}F NMR signals of $-2(CF_3)$ for compounds **1**, **2**, **3**, **4**, and **5** were observed at −77.38, −76.89, −76.71, −76.70, and −78.55 ppm, respectively.

FT-IR Spectra. The −OH stretching middle peaks of all complexes were absent in the FT-IR spectra; however, weak peaks were observed at ν = 2957 cm^{-1} (**1**), 2951 cm^{-1}(**2**), 2943 cm^{-1} (**3**), 2941 cm^{-1} (**4**), and 2940 cm^{-1} (**5**) (C−H stretching vibration); additionally, middle peaks were observed at ν = 1251 cm^{-1} (**1**), 1249 cm^{-1}(**2**), 1249 cm^{-1} (**3**), 1248 cm^{-1} (**4**), and 1250 cm^{-1} (**5**) ($Si-CH_3$ stretching vibration). This indicates that the trimethylsilylation of alcohol proceeded successfully in all compounds.

The FT-IR spectra exhibited C═O stretching peaks in coordinated β-diketones at 1654 cm^{-1} (**1**), 1652 cm^{-1}(**2**), 1651 cm^{-1} (**3**), 1656 cm^{-1} (**4**), and 1651 cm^{-1} (**5**), indicating that the reaction proceeded successfully.

Crystal Structure. X-ray-quality crystals of complexes **2**, **4**, and **5** were obtained from saturated toluene solutions at −30 °C. Complexes **2**, **4**, and **5** crystallized in monoclinic and triclinic space groups, where the silyl ether ligands exhibited a 5-membered ring structure (Figures 1, 2, and 3). All complexes exhibited a monomeric structure, where calcium and barium ions were bonded to two hfac ligands and coordinated to one silyl ether ligand, resulting in alcohol silylation from HMDS and meeH or tmgeH ligands. The metal-to-oxygen bonding distance of complex **4** was longer than that of complex **2**, which might be a result of high steric hindrance due to the presence of eight-coordinated oxygen atoms (Figure 2). The average O-M-O chelate angles of **3**, **4**, and **5** between the metal and mee or tmge ligands were 68.67°, 66.08°, and 59.06°, respectively (Figure 3). A gradual increase in bond angles between the metal and two hfac ligands was observed in the calcium (**4**), strontium, and barium (**5**) complexes (83.04, 86.77, and 88.90°, respectively).

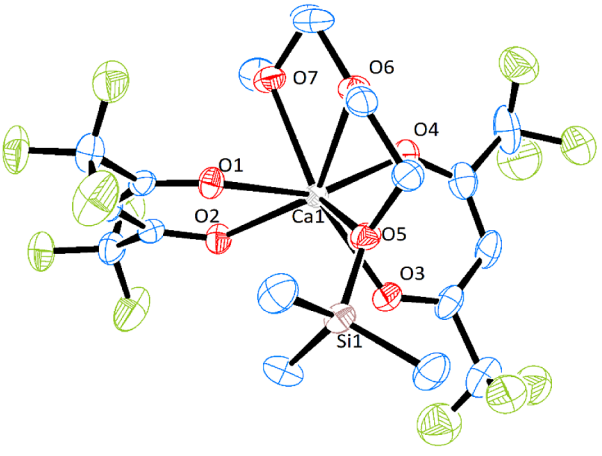

Figure 1. Crystal structure of $Ca(dts)(hfac)_2$ (**2**). Thermal ellipsoids are drawn at the 30% probability level and selected bond lengths (Å) and bond angles are represented in Table S2.

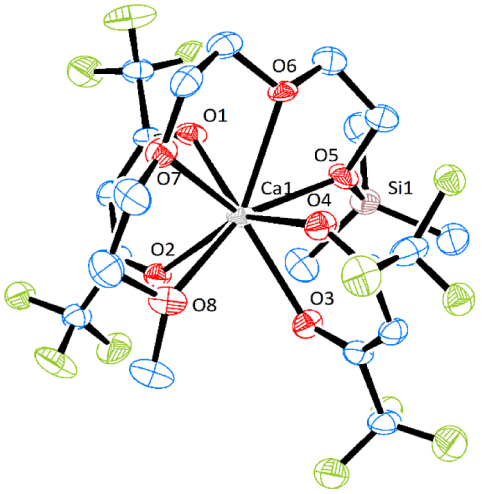

Figure 2. Crystal structure of $Ca(dmts)(hfac)_2$ (4). Thermal ellipsoids are drawn at the 30% probability level and selected bond lengths (Å) and bond angles are represented in Table S2.

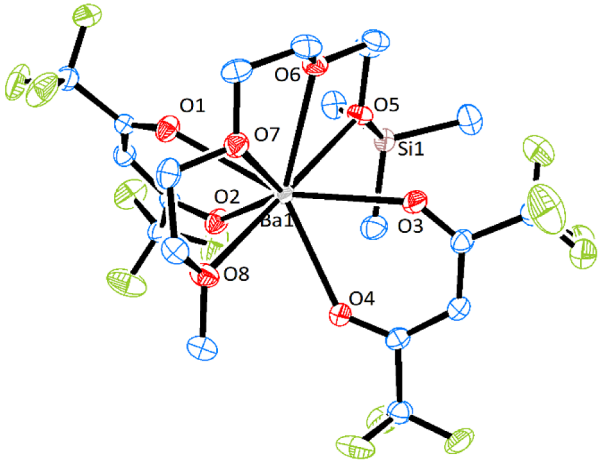

Figure 3. Crystal structure of $Ba(dmts)(hfac)_2$ (5). Thermal ellipsoids are drawn at the 30% probability level and selected bond lengths (Å) and bond angles are represented in Table S2.

DFT Calculation. The trimethylsilyl group shift was further investigated by DFT calculations using complex **4** as a representative model. The deprotonation and chelation of the tmgeH ligand and hfac ligands by chelated btsa ligands were highly exothermic processes (ΔG = −86.54, ΔG = −112.01, and −45.46 kcal/mol), as shown in Figure 4. During these processes, the deprotonated alcohol moiety in complexes **4a** and **4b** has the potential to react with HMDS via the S_N2 reaction pathway. However, a previous study using X-ray structural analysis showed that this moiety does not react with

https://doi.org/10.1021/acsomega.4c03479
ACS Omega 2024, 9, 31864−31870

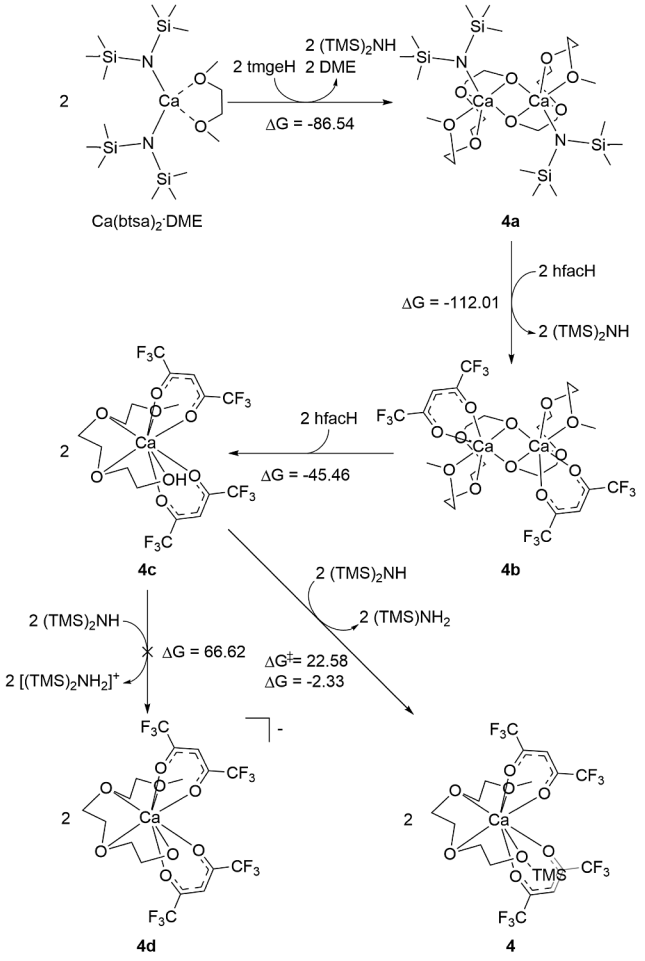

Figure 4. Proposed mechanism for the silylation of complex 4.

HMDS.[32] After the formation of complex **4c**, it was hypothesized that the reaction would proceed via a stepwise pathway. However, the energy difference between HMDS and complex **4c** of the acid−base reaction was large owing to the nonpolar solvent condition (ΔG = 66.62 kcal/mol). In contrast, the concerted reaction pathway proceeds with minimally charged intermediates in nonpolar solvents. This DFT study shows that the concerted reaction pathway may have a relatively low activation barrier with a minimal energy difference between the reactant and product ($\Delta G^{\ddagger}$ = 22.58 kcal/mol and ΔG = −2.33 kcal/mol). The driving force for this reaction was likely the electronegativity of the oxygen atom, which was higher than that of the nitrogen atom.[33]

TGA. Thermogravimetric analysis (TGA) of complexes **1**-**5** was conducted from room temperature to 600 °C under a constant flow of nitrogen to prevent air contact (Figure 5). A three-step mass-loss pattern was observed in the TGA curves of complexes **3** and **5**. In the first step (between 30 to 250 °C), TGA plots of complexes **3** and **5** exhibited 70 and 64% mass losses, respectively. During the other steps (between 250 and 500 °C), both complexes exhibited 21% and 20%, and residual masses of 9% and 16%, respectively; these values were similar to the mass percentages of MgO (5.93%) and BaO (19.4%). Complexes **1**, **3**, and **4** exhibited relatively sharp TGA curves between 35 and 228 °C; these complexes exhibited single-step weight losses of 99%, 97%, and 97.76% and residual masses of 1%, 2%, and 2%, respectively. Regarding magnesium,

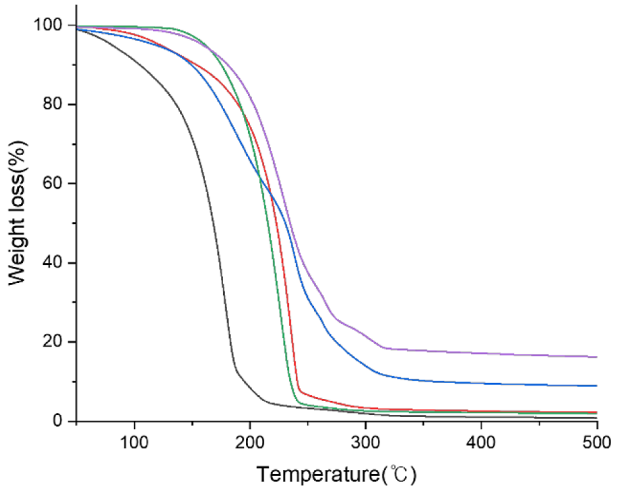

Figure 5. TGA plot of complexes 1 (black), 2 (red), 3 (blue), 4 (green), and 5 (purple).

complexes with mee ligand were more volatile than compounds with tmge ligand, whereas calcium complexes with tmge ligand tended to be more volatile than calcium complex with mee ligand. These differences likely occurred because of the difference in the coordination number between the elements, which is based on the atomic size. Theses complexes with high volatility can be used as ALD or CVD precursors to fabricate metal oxide thin films.

CONCLUSION

Novel group two β-diketonate complexes with ethereal or silyl groups were synthesized and characterized. All complexes were prepared via a controlled substitution reaction with $Mg(btsa)_2$·DME, $Ca(btsa)_2$·DME, and $Ba(btsa)_2$·2DME. Compounds **2**, **4**, and **5** exhibited monomeric structures with hepta- or octa-coordination states. In all complexes, the hydroxyl hydrogen of tmgeH and meeH was replaced by a trimethylsilyl group from HMDS as a byproduct. Si−CH_3 stretching vibration peaks were observed in the FT-IR spectra of all complexes. The TGA curves for complexes **1**, **2**, and **5** exhibited minimal nonvolatile residues and single-step weight losses. Using the DFT calculations of complex **4**, a possible reaction pathway for silylation was proposed based on the energy differences between each reaction intermediate. A concerted reaction pathway was favored because of the use of a nonpolar solvent; additionally, the difference in electronegativity between the oxygen and nitrogen atoms likely facilitated silylation.

EXPERIMENTAL SECTION

General Remarks. NMR spectra were recorded with a Bruker 500 MHz spectrometer (^{1}H, ^{13}C, and ^{19}F) with C_6D_6 as the solvent and reference. IR spectra were obtained using a Nicolet Nexus FT-IR spectrophotometer. Elemental analyses were carried out using a Thermo Scientific OEA Flash 2000 Analyzer. Thermogravimetric analyses were conducted using a SETARAM 92−18 TG-DTA instruments with a constant flow of nitrogen (500 mL/min) throughout the experiment. All reactions were carried out under inert dry conditions in an argon-filled glovebox. Hexane and toluene were purified using an Innovative Technology PS-MD-4 solvent purification system. All other chemicals were purchased from Aldrich and Alfa Aesar without further purification. $M[N(SiMe_3)]_2$·2L (*M*

https://doi.org/10.1021/acsomega.4c03479
ACS Omega 2024, 9, 31864−31870

= Mg, Ca, and Ba, L = DME) was prepared following previously reported methods.[34] Melting points were measured by the StuartTM SMP40 automatic melting point apparatus.

General Procedure for the Synthesis of Mg(dts)-(hfac)$_2$ and Ca(dts)(hfac)$_2$. A hexane solution (10 mL) of meeH (1 equiv) and hfacH (2 equiv) was added dropwise to a solution of Mg(btsa)$_2$·DME or Ca(btsa)$_2$·DME (1 equiv) in hexane (20 mL) at room temperature with constant stirring and stirred for 15 h. After the completion of the reaction, the reaction mixture was filtered and volatiles were removed in vacuo to obtain the product as a white solid. X-ray-quality crystals were grown from a saturated solution in toluene upon cooling.

Mg(dts)(hfac)$_2$ (**1**). Yield: 0.59 g (80%), ^{1}H NMR (500 MHz, C_6D_6): δ = 0.03 [s, 9H], 3.02 [s, 3H], 3.04 [t, 2H], 3.43 [t, 2H], 3.46−3.48 [m, 4H], 6.20 [s, 2H, β−C*H* (hfac)] ppm. ^{13}C NMR (125 MHz, C_6D_6): δ = −0.91, 59.07, 61.76, 70.01, 70.97, 73.38, 90.36, 117.14, 179.59 ppm. ^{19}F NMR (470.54 MHz, C_6D_6): δ = −77.38 ppm. FT-IR (ATR, cm^{-1}): 2957(w), 1654(m), 1512(m), 1472(w), 1251(m), 1196(m), 1138(s), 1059(m), 951(m), 842(m), 663(m), 584(w). $C_{18}H_{22}O_7Ca_1Si_1F_{12}$(630.73): C, 34.28; H, 3.52. Found: C, 34.71; H, 3.53.

Ca(dts)(hfac)$_2$ (**2**). Yield: 0.53 g (80%), mp 70 °C. ^{1}H NMR (500 MHz, C_6D_6): δ = 0.06 [s, 9H], 2.82 [s, 4H], 2.91 [m, 4H], 2.96 [s, 3H], 2.97 [t, 2H], 3.11 [s, 6H], 3.14 [t, 2H], 6.28 [s, 2H, β−C*H* (hfac)] ppm. ^{13}C NMR (125 MHz, C_6D_6): δ = −1.65, 58.88, 58.90, 61.80, 69.36, 70.55, 70.69, 71.63, 89.05, 117.56, 177.14 ppm. ^{19}F NMR (470.54 MHz, C_6D_6): δ = −76.89 ppm. FT-IR (ATR, cm^{-1}): 2951(w), 1652(m), 1524(m), 1469(w), 1249(m), 1185(m), 1131(s), 1047(m), 842(m), 793(m), 659(m), 526(w). $C_{18}H_{22}O_7Ca_1Si_1F_{12}$(646.52): C, 33.44; H, 3.43. Found: C, 33.45; H, 3.19.

General Procedure for the Synthesis of Mg(dmts)-(hfac)$_2$, Ca(dmts)(hfac)$_2$, and Ba(dmts)(hfac)$_2$. A hexane solution (10 mL) of tmgeH (1 equiv) and hfacH (2 equiv) was added dropwise to a solution of Mg(btsa)$_2$·DME or Ca(btsa)$_2$·DME or Ba(btsa)$_2$·2DME (1 equiv) in hexane (20 mL) at room temperature with constant stirring and was stirred for 15 h. After the completion of the reaction, the reaction mixture was filtered and volatiles were removed in vacuo to obtain the product as white solid. X-ray-quality crystals were grown from a saturated solution in toluene upon cooling.

Mg(dmts)(hfac)$_2$ (**3**). Yield: 0.50 g (75%). ^{1}H NMR (500 MHz, C_6D_6): δ = 0.06 [s, 9H], 2.96 [s, 3H], 3.01 [t, br, 2H], 3.34 [t, 4H], 3.45 [t, 2H], 3.48 [m, br, 4H], 6.23 [s, 2H] ppm. ^{13}C NMR (125 MHz, C_6D_6): δ = −0.61, 58.96, 61.97, 70.28, 70.54, 71.20, 72.97, 90.46, 116.81, 179.53 ppm. ^{19}F NMR (470.54 MHz, C_6D_6): δ = −76.71 ppm. FT-IR (ATR, cm^{-1}): 2943(w), 1738(w), 1651(m), 1509(s), 1471(m), 1249(m), 1186(m), 1130(s), 1076(m), 956(m), 848(s), 754(w), 575(m). $C_{20}H_{26}O_8Ca_1Si_1F_{12}$(674.52): C, 35.60; H, 3.88. Found: C, 35.27; H, 3.48.

Ca(dmts)(hfac)$_2$ (**4**). Yield: 0.59 g (80%), mp 100 °C. ^{1}H NMR (500 MHz, C_6D_6): δ = 0.04 [s, 9H], 2.67 [t, 2H], 2.84 [t, 2H], 3.08 [t, 2H], 3.10 [s, 3H], 3.14 [t, 2H], 3.22 [s, 2H], 3.27 [s, 2H], 6.31 [s, 2H, β−C*H* (hfac)] ppm. ^{13}C NMR (125 MHz, C_6D_6): δ = −1.50, 59.80, 62.24, 68.31, 69.73, 70.12, 71.11, 88.49, 119.96, 176.77 ppm. ^{19}F NMR (470.54 MHz, C_6D_6): δ = −76.70 ppm. FT-IR (ATR, cm^{-1}): 2941(w), 1656(m), 1516(m), 1495(w), 1248(m), 1178(m), 1136(s), 1075(m), 948(m), 846(m), 658(m), 578(w). $C_{20}H_{26}O_8Ca_1Si_1F_{12}$(690.58): C, 34.79; H, 3.79. Found: C, 33.31; H, 3.24.

Ba(dmts)(hfac)$_2$ (**5**). Yield: 0.61 g (78%), mp 110 °C. ^{1}H NMR (500 MHz, C_6D_6): δ = 0.03 [s, 9H], 2.80 [t, 2H], 2.93 [t, 2H], 2.97 [s, 3H], 3.03 [t, 2H], 3.08 [t, 2H], 3.25[t, 2H], 6.29 [s, 2H] ppm. ^{13}C NMR (125 MHz, C_6D_6): δ = −1.67, 58.66, 62.17, 69.77, 70.07, 70.95, 72.46, 88.07, 117.46, 175.83 ppm. ^{19}F NMR (470.54 MHz, C_6D_6): δ = −78.55 ppm. FT-IR (ATR, cm^{-1}): 2940(m), 1738(m), 1651(m), 1524(m), 1509(m), 1250(m), 1130(s), 1076(s), 956(w), 848(m), 790(m), 754(w), 693(m). $C_{20}H_{26}O_8Ba_1Si_1F_{12}$(787.84): C, 30.49; H, 3.33. Found: C, 30.52; H, 3.28.

Computational Details. The geometries were calculated in Orca 5.02 software[35] using the B3LYP functional.[36−39] Optimization and frequency calculation were proceeded using the def2-SVP basis set[40] with the auxiliary def2/J basis set[41] was used for all atoms. The single-point energy of optimized geometries was calculated using the def2-TZVPP basis set[40] with the auxiliary def2/J basis set[41] for all atoms. Each structure was confirmed by frequency calculations at the same level of theory to be a real local minimum on the potential energy surface. Solvation-free energies in hexane were calculated by using the polarizable continuum model (C-PCM) using Bondi atomic radii.[42−44]

■ ASSOCIATED CONTENT

Supporting Information

The Supporting Information is available free of charge at https://pubs.acs.org/doi/10.1021/acsomega.4c03479.

Crystallographic information for Complex 2(CIF)

Crystallographic information for Complex 3(CIF)

Crystallographic information for Complex 4(CIF)

The crystallographic data and data collection parameters selected bond lengths (Å) and bond angle (deg) for complexes **2**, **4**, **5** (Tables S1 and 2). ^{1}H NMR, ^{13}C NMR, and^{19}F-NMR spectrum of all Complexes (Figure S1−15). Optimized transition state structure for silylation of Complex **4** (Figure S16). Cartesian coordinates of all optimized structures (PDF)

■ AUTHOR INFORMATION

Corresponding Author

Taek-Mo Chung − *Thin Film Materials Research Center, Korea Research Institute of Chemical Technology, Daejeon 34114, Republic of Korea; Department of Chemical Convergence Materials, University of Science and Technology (UST), Daejeon 34113, Republic of Korea;* orcid.org/0000-0002-5169-2671; Email: tmchung@krict.re.kr

Authors

Chanwoo Park − *Thin Film Materials Research Center, Korea Research Institute of Chemical Technology, Daejeon 34114, Republic of Korea; Department of Chemistry, Korea University, Seoul 02841, Republic of Korea*

Seungjin Song − *Thin Film Materials Research Center, Korea Research Institute of Chemical Technology, Daejeon 34114, Republic of Korea*

Heenang Choi − *Thin Film Materials Research Center, Korea Research Institute of Chemical Technology, Daejeon 34114, Republic of Korea; Department of Chemistry, Sungkyunkwan University (SKKU), Gyeonggi-do 16419, Republic of Korea*

https://doi.org/10.1021/acsomega.4c03479
ACS Omega 2024, 9, 31864−31870

Bo Keun Park − *Thin Film Materials Research Center, Korea Research Institute of Chemical Technology, Daejeon 34114, Republic of Korea; Department of Chemical Convergence Materials, University of Science and Technology (UST), Daejeon 34113, Republic of Korea;* orcid.org/0000-0002-4066-0500

Ji Yeon Ryu − *Thin Film Materials Research Center, Korea Research Institute of Chemical Technology, Daejeon 34114, Republic of Korea;* orcid.org/0000-0001-6321-5576

Youngkwon Kim − *Thin Film Materials Research Center, Korea Research Institute of Chemical Technology, Daejeon 34114, Republic of Korea;* orcid.org/0000-0002-5788-8026

Complete contact information is available at: https://pubs.acs.org/10.1021/acsomega.4c03479

Author Contributions

#C.P., S.S. contributed equally.

Notes

The authors declare no competing financial interest.

■ ACKNOWLEDGMENTS

We are grateful to the Center for Chemical Analysis at the Korea Research Institute of Chemical Technology (KRICT) for allowing the use of their facilities and Bruker SMART APEX II for solving the crystal structures. This work was supported by the Development of smart chemical materials for IoT devices Project through the Korea Research Institute of Chemical Technology (KRICT) of Republic of Korea (KS2421-10).

■ REFERENCES

(1) Žurauskienė, N.; Balevičius, S.; Stankevič, V.; Paršeliūnas, J.; Keršulis, S.; Abrutis, A.; Plaušinaitienė, V. Influence of Sr Content on CMR Effect in Polycrystalline $La_{1-x}Sr_xMnO_3$ Thin Films. *Acta Phys. Polym., A* **2009**, *115*, 1136−1138.

(2) Nilsen, O.; Rauwel, E.; Fjellvåg, H.; Kjekshus, A. Growth of $La_{1-x}Ca_xMnO_3$ Thin Films by Atomic Layer Deposition. *J. Mater. Chem.* **2007**, *17*, 1466−1475.

(3) Caignaert, V.; Millange, F.; Domengès, B.; Raveau, B.; Suard, E. A New Ordered Oxygen-Deficient Manganite Perovskite: $LaBaMn_2O_{5.5}$. *Cryst. Magn. Struct. Chem. Mater.* **1999**, *11*, 930−938.

(4) Lo Nigro, R. L.; Toro, R. G.; Catalano, M. R.; Malandrino, G.; Fragalà, I. L.; Fiorenza, P.; Raineri, V. $CaCu_3Ti_4O_{12}$ Thin Films for Capacitive Applications: MOCVD Synthesis and Nanoscopic/Microscopic Characterization. *ECS Trans.* **2009**, *25*, 135−142.

(5) (a) Dimos, D. Ferroelectric Thin Films for Photonics: Properties and Applications. *Annu. Rev. Mater. Sci.* **1995**, *25* (25), 273−293. (b) Kaiser, D. L.; Vaudin, M. D.; Gillen, G.; Hwang, C.-S.; Robins, L. H.; Rotter, L. D. Growth and Characterization of Barium Titanate Thin Films Prepared by Metalorganic Chemical Vapor Deposition. *J. Cryst. Growth* **1994**, *137* (137), 136−140.

(6) Chen, J.; Wills, L. A.; Wessels, B. W.; Schulz, D. L.; Marks, T. J. Structure of organometallic chemical vapor deposited $BaTiO_3$ thin films on $LaAlO_3$. *J. Electron. Mater.* **1993**, *22* (6), 701−703.

(7) Van Buskirk, P. C.; Gardiner, R.; Kirlin, P. S.; Nutt, S. Reduced-Pressure MOCVD of Highly Crystalline $BaTiO_3$ Thin Films. *J. Mater. Res.* **1992**, *7*, 542−545.

(8) Pignard, S.; Yu-Zhang, K.; Leprince-Wang, Y.; Han, K.; Vincent, H.; Sénateur, J. P. Correlation Between Magnetoresistive Properties and Growth Morphology of $La_{1-x}MnO_{3-\delta}$ Thin Films Deposited on $SrTiO_3$, $LaAlO_3$ and MgO. *Thin Solid Films* **2001**, *391*, 21−27.

(9) Gorbenko, O. Y.; Bosak, A. A.; Kaul, A. R.; Babushkina, N. A.; Belova, L. M. Colossal Magnetoresisttve Tffin Films of (La 1-x ,Pr x) $_{0.7}$ Ca $_{0.3}$ MnO $_3$ Prepared by Aerosol MOCVD. *MRS Proc.* **1997**, *495*, 333−338.

(10) Snyder, G. J.; Hiskes, R.; DiCarolis, S.; Beasley, M. R.; Geballe, T. H. Intrinsic Electrical Transport and Magnetic Properties of $La_{0.67}Ca_{0.33}MnO_3$ and $La_{0.67}Sr_{0.33}MnO_3$ MOCVD Thin Films and Bulk Material. *Phys. Rev. B: Condens. Matter.* **1996**, *53*, 14434−14444.

(11) Lee, W.; Jeon, W.; An, C. H.; Chung, M. J.; Kim, H. J.; Eom, T.; George, S. M.; Park, B. K.; Han, J. H.; Kim, C. G.; et al. Improved Initial Growth Behavior of SrO and $SrTiO_3$ Films Grown by Atomic Layer Deposition Using $\{Sr(Demamp)\ (tmhd)\}_2$ as Sr-Precursor. *Chem. Mater.* **2015**, *27*, 3881−3891.

(12) Malghe, Y. S.; Gurjar, A. V.; Dharwadkar, S. R. Synthesis of $BaTiO_3$ Powder from Bariumtitanyl Oxalate (BTO) Precursor Employing Microwave Heating Technique. *Bull. Mater. Sci.* **2004**, *27*, 217−220.

(13) Win, T.; Naing, K.; Tun, K. M. Synthesis of Barium Titanate from Titanyl Acylate Precursor by Sol-Precipitate Method. *J. Myanmar Acad., Arts Sci.* **2008**, *6*, 61−70.

(14) Hatanpää, T.; Vehkamäki, M.; Mutikainen, I.; Kansikas, J.; Ritala, M.; Leskelä, M. Synthesis and Characterisation of Cyclopentadienyl Complexes of Barium: Precursors for Atomic Layer Deposition of $BaTiO_3$. *Dalton Trans.* **2004**, *8*, 1181−1188.

(15) Acharya, S.; Torgersen, J.; Kim, Y.; Park, J.; Schindler, P.; Dadlani, A. L.; Winterkorn, M.; Xu, S.; Walch, S. P.; Usui, T.; et al. Self-Limiting Atomic Layer Deposition of Barium Oxide and Barium Titanate Thin Films Using a Novel Pyrrole Based Precursor. *J. Mater. Chem. C* **2016**, *4*, 1945−1952.

(16) Daly, S. R.; Bellott, B. J.; Nesbit, M. A.; Girolami, G. S. Synthesis and Structural Diversity of Barium (N,N-dimethylamino)-Diboranates. *Inorg. Chem.* **2012**, *51*, 6449−6459.

(17) Oh, S. H.; Ko, J. H.; Lee, H. Y.; Lazar, I.; Roleder, K. Precursor Phenomena of Barium Titanate Single Crystals Grown Using a Solid-State Single Crystal Growth Method Studied with Inelastic Brillouin Light Scattering and Birefringence Measurements. *Molecules* **2018**, *23*, 3171−3184.

(18) De, R.; Maidul Haque, S.; Tripathi, S.; Rao, K. D.; Prathap, C.; Kumar, M.; Som, T.; Sahoo, N. K. Surface characterization of magnesium fluoride thin films prepared by a fluorine trapping based non-reactive sputtering technique. *Vacuum* **2016**, *134*, 110−119.

(19) Adamik, M.; Sáfrán, G.; Barna, P. B.; Laux, S.; Richter Thin Solid, W. Growth Structure Investigation of MgF_2 and NdF_3 Films Grown by Molecular Beam Deposition on $CaF_2(111)$ substrates. *Thin Solid Films* **1996**, *280*, 5−15.

(20) Tiitta, M.; Niinistou, L. Volatile Metal β-Diketonates: ALE and CVD Precursors for Electroluminescent Device Thin Films. *Chem. Vap. Deposition* **1997**, *3*, 167−182.

(21) Wojtczak, W. A.; Fleig, P. F.; Hampden-Smith, M. J. A Review of Group 2 (IIA) (Ca, Sr, Ba) Metal-Organic Compounds as Precursors for Chemical Vapor Deposition. *Adv. Organomet. Chem.* **1996**, *40*, 215−340.

(22) Schulz, D. L.; Marks, T. J. MOCVD Routes to Thin Metal Oxide Films for Superconducting Electronics. *Adv. Mater.* **1994**, *6*, 719−730.

(23) Wessels, B. W. Metal-Organic Chemical Vapor Deposition of Ferroelectric Oxide Thin Films for Electronic and Optical Applications. *Annu. Rev. Mater. Sci.* **1995**, *25*, 525−546.

(24) Pilvi, T.; Ritala, M.; Leskelä, M.; Bischoff, M.; Kaiser, U.; Kaiser, N. Atomic Layer Deposition Process with TiF_4 as a Precursor for Depositing Metal Fluoride Thin Films. *Appl. Opt.* **2008**, *47*, C271−C274.

(25) Pilvi, T.; Hatanpää, T.; Puukilainen, E.; Arstila, K.; Bischoff, M.; Kaiser, U.; Kaiser, N.; Leskelä, M.; Ritala, M. Study of a Novel ALD Process for Depositing MgF_2 Thin Films. *J. Mater. Chem.* **2007**, *17*, 5077.

(26) Aarik, J.; Aidla, A.; Jaek, A.; Leskelä, M.; Niinistö, L. Precursor properties of calcium β-diketonate in vapor phase atomic layer epitaxy. *Appl. Surf. Sci.* **1994**, *75*, 33−38.

(27) Ylilammi, M.; Ranta-Aho, T. Metal Fluoride Thin Films Prepared by Atomic Layer Deposition. *J. Electrochem. Soc.* **1994**, *141*, 1278.
(28) Guillon, H.; Hubert-Pfalzgraf, L. G.; Vaisserman, J. S. SYNTHESIS, CHARACTERIZATION AND THERMAL BEHAVIOUR OF CALCIUM AND STRONTIUM 2, 2, 6, 6-TETRAMETHYL-3,5-HEPTANEDIONATE COMPLEXES. CRYSTAL STRUCTURE OF $[Sr(\mu, \eta^2\text{-thd})(\eta^2\text{-thd})(\eta^2\text{-MeOC}_2H_4OH)]_2$. *Main Group Met. Chem.* **1997**, *20* (10), 633−639.
(29) Kosola, A.; Putkonen, M.; Johansson, L.-S.; Niinistö, L. Effect of annealing in processing of strontium titanate thin films by ALD. *Appl. Surf. Sci.* **2003**, *211*, 102.
(30) Tammenmaa, M.; Antson, H.; Asplund, M.; Hiltunen, L.; Leskelä, M.; Niinistö, L.; Ristolainen, E. Ristolainen, Alkaline earth sulfide thin films grown by atomic layer epitaxy. *J. Cryst. Growth* **1987**, *84*, 151.
(31) Saanila, V.; Ihanus, J.; Ritala, M.; Leskelä, M. Atomic Layer Epitaxy Growth of BaS and BaS: Ce Thin Films from In Situ Synthesized $Ba(thd)_2$. *Chem. Vap. Deposition* **1998**, *4*, 227.
(32) Park, C.; Choi, H.; Lee, G. Y.; Park, B. K.; Ryu, J. Y.; Chung, T.-M. Synthesis of Mononuclear Strontium Complexes with Polyether and β-DiketonatoLigands. *ACS Omega* **2023**, *8*, 16119−16130.
(33) Dean, J. A. *Lange's handbook of chemistry*; McGraw-HILL, 1999.
(34) Westerhausen, M. Synthesis and spectroscopic properties of bis(trimethylsilyl)amides of the alkaline-earth metals magnesium, calcium, strontium, and barium. *Inorg. Chem.* **1991**, *30*, 96−101.
(35) Neese, F. The ORCA program system *Wiley Interdiscip. Rev. Comput. Mol. Sci.* **2012**, *2*, 73−78.
(36) Becke, A. D. A new mixing of Hartree−Fock and local density-functional theories. *J. Chem. Phys.* **1993**, *98*, 1372−1377.
(37) Becke, A. D. Density-functional thermochemistry. III. The role of exact exchange. *J. Chem. Phys.* **1993**, *98*, 5648−5652.
(38) Becke, A. D. Density-functional exchange-energy approximation with correct asymptotic behavior. *Phys. Rev. A* **1988**, *38*, 3098−3100.
(39) Lee, C.; Yang, W.; Parr, R. G. Development of the Colle-Salvetti correlation-energy formula into a functional of the electron density. *Phys. Rev. B* **1988**, *37*, 785−789.
(40) Weigend, F.; Ahlrichs, R. Balanced basis sets of split valence, triple zeta valence and quadruple zeta valence quality for H to Rn: Design and assessment of accuracy. *Phys. Chem. Chem. Phys.* **2005**, *7*, 3297−3305.
(41) Weigend, F. Accurate Coulomb-fitting basis sets for H to Rn. *Phys. Chem. Chem. Phys.* **2006**, *8*, 1057−1065.
(42) Barone, V.; Cossi, M. Quantum calculation of molecular energies and energy gradients in solution by a conductor solvent model. *J. Phys. Chem. A* **1998**, *102*, 1995−2001.
(43) Cossi, M.; Rega, N.; Scalmani, G.; Barone, V. Energies, structures, and electronic properties of molecules in solution with the C-PCM solvation model. *J. Comput. Chem.* **2003**, *24*, 669−681.
(44) Bondi, A. van der Waals volumes and radii. *J. Phys. Chem.* **1964**, *68*, 441−451.

https://doi.org/10.1021/acsomega.4c03479
ACS Omega 2024, 9, 31864−31870